



Active targeting and safety profile of PEG-modified adenovirus conjugated with herceptin

Pyung-Hwan Kim^{a,1}, Joo-Hyuk Sohn^{b,1}, Joung-Woo Choi^a, Yukyung Jung^c, Sung Wan Kim^{d,e},
Seungjoo Haam^{a,c,*}, Chae-Ok Yun^{a,b,**}

^a Graduate Program for Nanomedical Science, Yonsei University, 134 Shinchon-Dong, Seodaemun-Gu, Seoul 120-749, South Korea

^b Brain Korea 21 project for Medical Science, Institute for Cancer Research, Severance Biomedical Science Institute, Yonsei University College of Medicine, 134 Shinchon-Dong, Seodaemun-Gu, Seoul 120-749, South Korea

^c Department of Chemical Engineering, Yonsei University, 134 Shinchon-Dong, Seodaemun-Gu, Seoul 120-749, South Korea

^d Department of Pharmaceutics and Pharmaceutical Chemistry, University of Utah, Salt Lake City, UT 84112, USA

^e Department of Bioengineering, College of Engineering, Hanyang University, Seoul, South Korea

ARTICLE INFO

Article history:

Received 28 September 2010

Accepted 15 October 2010

Available online 11 January 2011

Keywords:

Cancer gene therapy

Adenovirus

Ad conjugated bioreducible polymer

Hybrid vector

Active targeting

ABSTRACT

PEGylation of adenovirus (Ad) increases plasma retention and reduces immunogenicity, but decreases the accessibility of virus particles to target cells. We tested whether PEGylated Ad conjugated to Herceptin (Ad-PEG-HER) can be used to treat Her2/neu-positive cells *in vitro* and *in vivo* to demonstrate the therapeutic feasibility of this Ad formulation. Ad-PEG-HER transduced Her2/neu-overexpressing cancer cells through a specific interaction between Herceptin and Her2/neu. Ad-PEG-HER treatment resulted in higher plasma retention and lower neutralizing antibody and IL-6 production than naked Ad. This formulation was extended to generate a Her2/neu-targeted, PEGylated oncolytic Ad (DWP418-PEG-HER). DWP418-PEG-HER specifically killed Her2/neu-positive cells and performed better than non-targeted and naked Ad *in vivo*. DWP418-PEG-HER showed a 10^{10} -fold increase in the liver to tumor biodistribution compared with naked Ad. Immunohistochemical staining confirmed accumulation of Ad E1A in tumors. These data suggest that targeted gene therapy with the PEGylated Ad conjugated with Herceptin might shed a light on its therapeutic application for metastatic cancer in the future.

© 2010 Elsevier Ltd. All rights reserved.

1. Introduction

The primary goals of gene therapy are to develop vectors and delivery systems that achieve efficient *in vivo* gene transfer and expression [1]. Of the viral vectors being developed for gene therapy purposes, the adenovirus (Ad) system has shown considerable promise and has undergone extensive evaluation in animal models and clinical trials for the treatment of cancer [2,3]. In particular, oncolytic Ad has advantages for cancer therapy, such as self-propagation, lysis of infected cancer cells, and secondary infection of adjacent cells within the tumor. The use of oncolytic Ad as a cancer therapeutic has already been approved for a randomized phase III trial in China [4–6]. However, systemically

administered Ad vectors suffer from a short retention time in the blood and trapping in the liver, and these characteristics must be eliminated to develop a successful therapeutic Ad vector.

Polyethylene glycol (PEG) is an uncharged, hydrophilic, non-immunogenic polymer that is known to be able to reduce protein–protein interactions [7]. Modification of Ad virions with PEG (PEGylation) has been investigated to improve Ad retention time and prevent trapping in the liver. PEGylation of Ad substantially reduces immunologic clearance of Ad, leading to increase blood retention time [7–10]. However, PEGylation reduces the efficiency of Ad gene delivery due to a decreased ability of the virus to bind to and be internalized by host cells. To overcome this limitation, cell-specific retargeting moieties, such as RGD peptide, folate ligand, and transferrin, have been investigated [11–16]. While previous studies have shown efficient ligand-specific Ad gene transfer *in vitro*, targeted antitumor efficacy *in vivo* after systemic administration of Ad has yet to be demonstrated. Several cell surface tumor biomarkers have been investigated as potential ligands for Ad targeting [17,18]. Her2/neu is a human epidermal growth factor 2 receptor known to be overexpressed in 20–30% of breast cancer

* Corresponding author. Yonsei University, 134 Shinchon-Dong, Seodaemun-Gu, Seoul, South Korea. Tel.: +82 2 2123 2751; fax: +82 2 312 6401.

** Corresponding author. Yonsei University, College of Medicine, 134 Shinchon-Dong, Seodaemun-Gu, Seoul, South Korea. Tel.: +82 2228 8040; fax: +82 2227 7751.

E-mail addresses: ham@yonsei.ac.kr (S. Haam), chaek@yuhs.ac (C.-O. Yun).

¹ These authors contributed equally to this work.

patients. Her2/neu has a crucial role as an oncogene in these cancers, and drugs targeting Her2/neu, such as trastuzumab and lapatinib, are in clinical use [19,20]. Trastuzumab (Herceptin), a Her2/neu-specific monoclonal antibody is also being used widely to treat both metastatic and early breast cancer [21,22].

To test the specific targeting of PEGylated Ad to Her2/neu-positive cancer cells *in vitro* and *in vivo*, we constructed a ternary Ad vector conjugate consisting of a replication-deficient Ad that is PEGylated and conjugated to Herceptin (Ad-PEG-HER). We previously demonstrated that Ad-PEG-HER specifically transduces Her2/neu-positive cancer cells [23]. Further, in parallel with the development of targeted delivery systems, endeavours to increase the specificity and potency of therapeutic Ad vectors led to the use of an oncolytic Ad (DWP418) in a phase I clinical trial. Tumor-cell specific DWP418 replication is controlled by the use of the telomerase reverse transcriptase (TERT) promoter within the virus genome and is reinforced by deleting the E1B19 portion of the virus and inserting a relaxin gene [24–26]. The goal of this study is to demonstrate proof-of-concept for the development of a targeted oncolytic Ad vector that is PEGylated and conjugated to Herceptin, can be administered systemically, and will selectively accumulate within and kill Her2/neu-positive cancer cells *in vitro* and established tumors *in vivo*.

2. Materials and methods

2.1. Cell culture, generation of the Ad, and synthesis of Ad-PEG and Ad-PEG-HER conjugates

All cell lines were cultured in Dulbecco's modified Eagle's medium (DMEM; GIBCO-BRL, Grand Island, NY) supplemented with 10% fetal bovine serum (FBS) (GIBCO-BRL) at 37 °C in a humidified atmosphere containing 5% CO₂. A human embryonic kidney cell line (HEK 293) expressing the Ad E1 region, Her2/neu-expressing human breast cancer lines MDA-MB231 and MDA-MB435, Her2/neu-expressing human ovarian cancer cell line SK-OV3, Her2/neu-negative human breast cancer cell line MCF7-mot, human hepatoma cell line SK-Hep1, human brain cancer cell line U343, human cervical cancer cell line HeLa, and human normal fibroblast cell line IMR90 were purchased from the American Type Culture Collection (ATCC, Manassas, VA). For the replication-deficient Ad, E1-deleted Ad type 5 expressing GFP under the control of cytomegalovirus (CMV) promoter inserted into the E1 region of Ad (dE1/GFP) was generated as previously described [23]. Replication-competent Ad used was a modified human telomerase reverse transcriptase (mTERT) promoter-regulated oncolytic Ad where the E1B19 kDa portion of the virus was deleted and a relaxin gene was inserted into the E3 region to increase the oncolytic potency as described in previous reports [24,26]. PEGylation of Ad and conjugation of Herceptin into dE1/GFP and DWP418 was performed and validated as previously described [23].

2.2. Competition assay

SK-OV3 cells were seeded onto 24-well plates at 1×10^5 cells per well. On the following day, either RMCB (2, 5 mg/ml) or Herceptin (5 mg/ml) in serum-free DMEM or equivalent amount of phosphate-buffered saline (PBS) was administered for 1 h at 4 °C before naked Ad (dE1/GFP), Ad-PEG, or Ad-PEG-HER transduction. After 2 h at room temperature, unbound virus was rinsed off. Cells were incubated for 48 h at 37 °C and observed by fluorescence microscopy (Olympus BX51; Olympus Optical, Tokyo, Japan) using the MetaMorph Imaging System (Molecular Devices, Sunnyvale, CA). GFP expression was quantified by flow cytometry analysis and analyzed using the CellQuest software (Beckton-Dickinson, Sunnyvale, CA).

2.3. Assays for neutralizing antibody and interleukin-6 (IL-6)

BALB/c mice were maintained in a laminar airflow cabinet under specific pathogen-free conditions. All facilities are approved by the Association and Accreditation of Laboratory Animal Care (AAALAC) and all animal-related experiments were conducted under the institutional guidelines established for the animal core facility at Yonsei University College of Medicine. A single dose of 1×10^{10} viral particles (VP) of naked Ad, Ad-PEG, or Ad-PEG-HER was administered intravenously to female BALB/c mice (Charles River Korea Inc., Seoul, Korea), and 14 days later, naked Ad, Ad-PEG, or Ad-PEG-HER was re-administered. Whole blood was collected from the retro-orbital vein at 14 days after 2nd injection. Then, mouse serum was heat-inactivated at 56 °C for 45 min to inactivate complement and stored at –20 °C. For the neutralization protection assay, each heat-inactivated serum from naked Ad-, Ad-PEG-, or Ad-PEG-HER-treated mice was diluted 1:50 in PBS with 1% FBS,

mixed with dE1/GFP, and incubated for 20 min at 37 °C. These serum-treated Ads were added to U343 cell that were 80% confluent in 24-well plates at a multiplicity of infection (MOI) of 400 and incubated for 2 h at 37 °C. The cells were washed, incubated with 1 ml medium with 5% FBS for 48 h, and then scored for infection by fluorescence microscopy (Olympus BX51) using the MetaMorph Imaging System (Molecular Devices). In addition, cells were further analyzed using a FACScan flow cytometer and CellQuest software (Beckton-Dickinson). To determine the effects of each Ad formulation on the acute innate response, serum IL-6 from mice systemically injected with naked Ad, Ad-PEG, or Ad-PEG-HER (1×10^{10} VP/mouse) was measured. Serum samples were collected at 6 h post-injection and serum IL-6 levels were then quantified using an IL-6 ELISA (R&D Systems, Minneapolis, MN).

2.4. Determination of Ad clearance from blood

To assess the rate of Ad clearance from the blood of BALB/c mice, real-time quantitative PCR was performed on whole blood samples. In brief, 100 µl of whole blood was collected from the retro-orbital plexus at 5, 10, 20, 30, 40, and 60 min post-injection with 1×10^{10} VP of naked Ad, Ad-PEG, and Ad-PEG-HER into the tail vein. Total DNA, including Ad DNA, from an aliquot of whole blood was extracted and resuspended in a final volume of 50 µl using the QIAamp DNA blood mini kit (Qiagen, Hilden, Germany) according to the manufacturer's instructions. The number of Ad genomes was measured by real-time quantitative PCR (TaqMan PCR detection; Applied Biosystems, Foster City, CA). A fluorogenic probe (FAM-5'-CCGCCGCTTCAGCC-3'-NFQ) was designed to anneal to the target sequence between the sense primer (5'-GGAACGCGTTGGAGACT-3') and the antisense primer (5'-GGAAGCAAAGTCAGTCACAATCC-3') in the IX protein region of the Ad genome. Samples were amplified for 40 cycles in an ABI 7500 sequence detection system (Applied Biosystems) with continuous fluorescence monitoring. All samples were analyzed in triplicate and data were processed by the SDS 19.1 software package (Applied Biosystems).

2.5. MTT assay

To evaluate the cytopathic effect of oncolytic Ad, SK-OV3, MDA-MB231, SK-Hep1 and IMR90 cells grown to 30–70% confluence in 24-well plates were infected with naked DWP418, DWP418-PEG, or DWP418-PEG-HER at MOIs ranging from 10 to 500 and incubated at 37 °C. Four days post infection, 200 µl of 3-(4,5-dimethylthiazol-2-yl)-2,5-diphenyl-tetrazolium bromide (MTT; Sigma Chemical Corp) at 2 mg/ml in PBS was added to each well. The cells were incubated at 37 °C for 4 h, then the supernatant was discarded and the precipitate dissolved in 1 ml dimethylsulfoxide (DMSO). Plates were then read on a microplate reader at 540 nm. The number of living cells in a non-infected cell group was analyzed similarly as a negative control.

2.6. In vivo anti-tumor effects

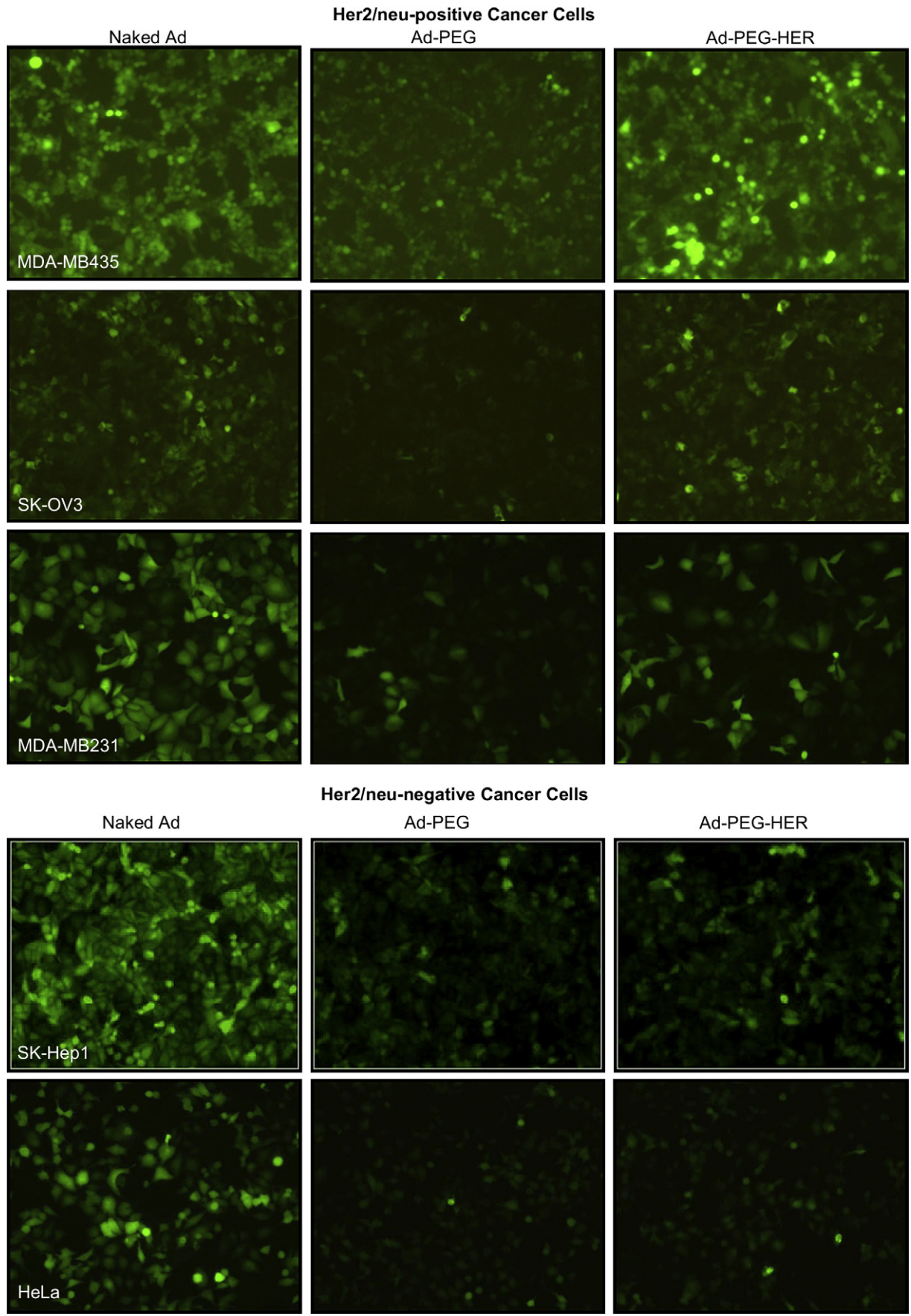
To assess the antitumor effect of naked DWP418, PEGylated DWP418 (DWP418-PEG), and Herceptin-conjugated and PEGylated DWP418 (DWP418-PEG-HER), xenograft tumors of SK-OV3, MDA-MB435, or MCF7-mot cells were established subcutaneously by injecting 1×10^7 cells into abdomen of 6- to 8-week-old female athymic nude mice (Charles River Korea Inc). Once the tumors reached 100–120 mm³ in volume, mice were randomized into four groups and injected intravenously with 100 µl PBS or 2.5×10^{10} VP (for SK-OV3), 1×10^{10} VP (for MDA-MB435), or 2×10^{10} VP (for MCF7-mot) of naked DWP418, DWP418-PEG, or DWP418-PEG-HER in 100 µl of PBS three times every other day. Tumor growth was measured three times weekly using a caliper until the end of study. The length and width of the tumor was measured and the tumor volume was calculated according to the following formula: tumor volume = 0.523 Lw^2 .

2.7. Ad biodistribution assessment by real-time quantitative PCR

Once the MDA-MB435 tumor volume had reached approximately 100–150 mm³ in size, tumor-bearing mice were injected intravenously with 1×10^{10} VP of naked DWP418, DWP418-PEG, or DWP418-PEG-HER three times every other day. The tumor, heart, kidney, lung, stomach, muscle, and liver were harvested 24 h after the third injection, and DNA was extracted from the tissues using the QIAamp DNA blood mini kit (Qiagen) according to the manufacturer's instructions. The number of viral genomes in each sample was assessed by real-time quantitative PCR, as described above.

2.8. Assessment of in vivo toxicity

To measure *in vivo* toxicity of the Ad formulations, 1×10^{10} VP of naked DWP418, DWP418-PEG, or DWP418-PEG-HER were injected intravenously into each mouse. Serum levels of aspartate aminotransferase (AST) and alanine transaminase (ALT) were then measured 3 days post-injection. Subsequently, the animals were sacrificed, and liver tissues were embedded in paraffin for hematoxylin and eosin staining or frozen in optimal cutting temperature (OCT) freezing medium for E1A and relaxin immunodetection. E1A immunodetection was performed by incubating the OCT embedded liver sections with an Ad E1A-specific polyclonal antibody (clone



13 S-5; Santa Cruz Biotechnology, Heidelberg, Germany). AlexaFluor 488-labeled goat anti-rabbit antibody (Molecular Probes, Eugene, OR) was used as a secondary antibody. The nuclei were counterstained with 5 µg/ml bis-benzimide (Hoechst 33342; Sigma) and visualized using a fluorescent microscope (Observer/Z1; Zeiss, Barcelona, Spain). Images were captured using a digital camera (AxioCamMRm; Zeiss).

2.9. Statistical analysis

The data are expressed as the mean ± standard error of the mean (SEM). Statistical comparisons were performed using the Mann–Whitney test. The criterion for statistical significance was P values < 0.05.

3. Results

3.1. Her2/neu-targeted entry of PEGylated Ad conjugated with Herceptin

We previously reported the construction, characterization, and validation of PEGylated Ad conjugated to Herceptin (Ad-PEG-HER) [23]. In that work, a replication-deficient Ad vector was used. Here, we utilized the same construction process and fast performance liquid chromatography (FPLC)-purified virus to develop a similar Ad-PEG-HER formulation but using the replication-competent oncolytic Ad, and virus number was titrated using the real-time quantitative PCR during the course of the experiments.

First, we sought to determine whether Ad-PEG-HER could specifically transduce cells in a Her2/neu-specific manner. Her2/neu-positive (MDA-MB435, SK-OV3, and MDA-MB231) and Her2/neu-negative (SK-Hep1 and HeLa) cells were treated with naked Ad, PEGylated Ad (Ad-PEG), or Ad-PEG-HER. As shown in Fig. 1, GFP expression in Ad-PEG-treated cells was much less than in naked Ad-treated cells, indicating the transduction efficiency of Ad-PEG was substantially lower than that with naked Ad in both Her2/neu-positive and Her2/neu-negative cells. This is due to physical blocking of the Ad fiber protein by PEG conjugation. In contrast, transduction efficiency by Ad-PEG-HER was similar to transduction by naked Ad in Her2/neu-positive cells, but GFP expression in Ad-PEG-HER-treated cells was significantly reduced in Her2/neu-negative SK-Hep1 and HeLa cells. The GFP expression in Ad-PEG-HER-treated Her2/neu-negative cells was similar to Ad-PEG treated cells, which indicated entry of Ad-PEG-HER primarily depended on Her2/neu cell surface expression.

To demonstrate that Ad-PEG-HER transduction was dependent on Her2/neu and independent of the coxsackievirus and adenovirus receptor (CAR), SK-OV3 cells, which express both Her2/neu and CAR were pre-incubated with CAR-specific (RMCB) or Her2/neu-specific (Herceptin) antibodies prior to transduction (Fig. 2 a,b). Pretreatment with CAR-specific RMCB substantially reduced GFP transduction with naked Ad in a dose-dependent manner (43% and 61% decreases with 2 and 5 mg/ml RMCB antibody pretreatment, respectively). In contrast, GFP transduction mediated by Ad-PEG-HER was not blocked by RMCB, indicating that Ad-PEG-HER uptake was not mediated by interaction between CAR and fiber (Fig. 2 a). When cells were pre-treated with the Her2/neu-specific monoclonal antibody Herceptin, GFP transduction by Ad-PEG-HER was 48% lower than in non-treated cells, but Herceptin had no effect on GFP transduction by naked Ad (Fig. 2 b). Thus, these data show that entry of Ad-PEG-HER is mediated by a Her2/neu-dependent pathway and independent of the normal CAR-mediated pathway.

3.2. Reduced innate and humoral immune response against PEGylated Ads

Virus vectors typically activate the innate immune system, but *in vivo* gene delivery vectors must have attenuated immune activation. We assessed changes in the serum level of the proinflammatory cytokine IL-6 induced by each Ad preparation as a measure of innate immune system activation. BALB/c mice were treated intravenously with 1×10^{10} VP of naked Ad, Ad-PEG, or Ad-PEG-HER and 6 h post-injection sera from mice was harvested and the IL-6 level analyzed by ELISA. As shown in Fig. 3 a, injection of naked Ad dramatically increased serum IL-6 levels (411 pg/ml), which was approximately 9-fold higher than PBS-treated mice (46 pg/ml, $P < 0.01$). Intravenous injection of Ad-PEG or Ad-PEG-HER did not substantially increase serum IL-6 levels, which were significantly lower than in naked Ad-treated animals (14 pg/ml for Ad-PEG; 77 pg/ml for Ad-PEG-HER) (Fig. 4).

Next, we determined whether PEGylation of Ad masks virus epitopes and blocks induction of neutralizing antibodies. Mice were treated intravenously with 1×10^{10} VP of naked Ad, Ad-PEG, or Ad-PEG-HER. To determine if these mice developed neutralizing antibodies, U343 cells were transduced with a GFP-expressing Ad (dE1/GFP) in the presence of serum from the Ad vector-treated mice or non-immune serum as a negative control. A 1:50 dilution of serum from a mouse treated with naked Ad reduced the transduction efficiency of dE1/GFP by 95% (Fig. 3 b). In contrast, dE1/GFP transduction efficiency in the presence of serum from mice injected with Ad-PEG or Ad-PEG-HER was only reduced by 36% and 30%, respectively. Thus, PEGylation of Ad reduced the ability of these vectors to induce Ad-specific neutralizing antibodies by the recipient.

3.3. Pharmacokinetic profiles of naked Ad, Ad-PEG, and Ad-PEG-HER

We next examined the pharmacokinetics of each Ad vector preparation. Balb/C mice were treated intravenously with 1×10^{10} VP of naked Ad, Ad-PEG, and Ad-PEG-HER, and the clearance of the virus from the blood was determined by quantitating the number of viral gene copies over time using real-time quantitative-RT-PCR. Naked Ad was rapidly cleared from blood by 10 min post-injection, with steady-state retention of 1.36×10^5 VP. In contrast, Ad-PEG and Ad-PEG-HER maintained higher levels, with 6.15×10^6 and 2.1×10^6 VP of Ad-PEG and Ad-PEG-HER detected, respectively. This was a 45-fold and 16-fold increase over naked Ad, respectively. Further, the PEGylated virus was retained at 5- to 6-fold higher levels even 1 h after injection. These results indicate that PEG conjugation significantly increased the blood circulation time of Ad, and addition of the Herceptin targeting moiety did not negatively affect this PEG-mediated increase in blood circulation time.

3.4. Her2/neu-specific cell killing of PEG-modified oncolytic Ad conjugated with Herceptin

To explore Her2/neu-specific cancer cell killing, we modified a novel oncolytic Ad, DWP418, with PEG and Herceptin. Replication of this virus is controlled by a modified TERT promoter and contains the relaxin gene. We previously demonstrated that the modified TERT promoter-regulates oncolytic Ad replication by supporting replication only in cells with high telomerase activity,

Fig. 1. Her2/neu-specific transduction by Ad-PEG-HER. (a) Her2/neu-positive (MDA-MB435, SK-OV3, and MDA-MB231) and -negative (SK-Hep1 and HeLa) cells were transduced with naked Ad, Ad-PEG, or Ad-PEG-HER. GFP was observed by fluorescence microscopy at 48 h after transduction. The transduction of Ad-PEG-HER was dependent on the expression of Her2/neu, whereas Ad-PEG showed significantly lower transduction efficiency compared with naked Ad in both Her2/neu-positive and -negative cells.

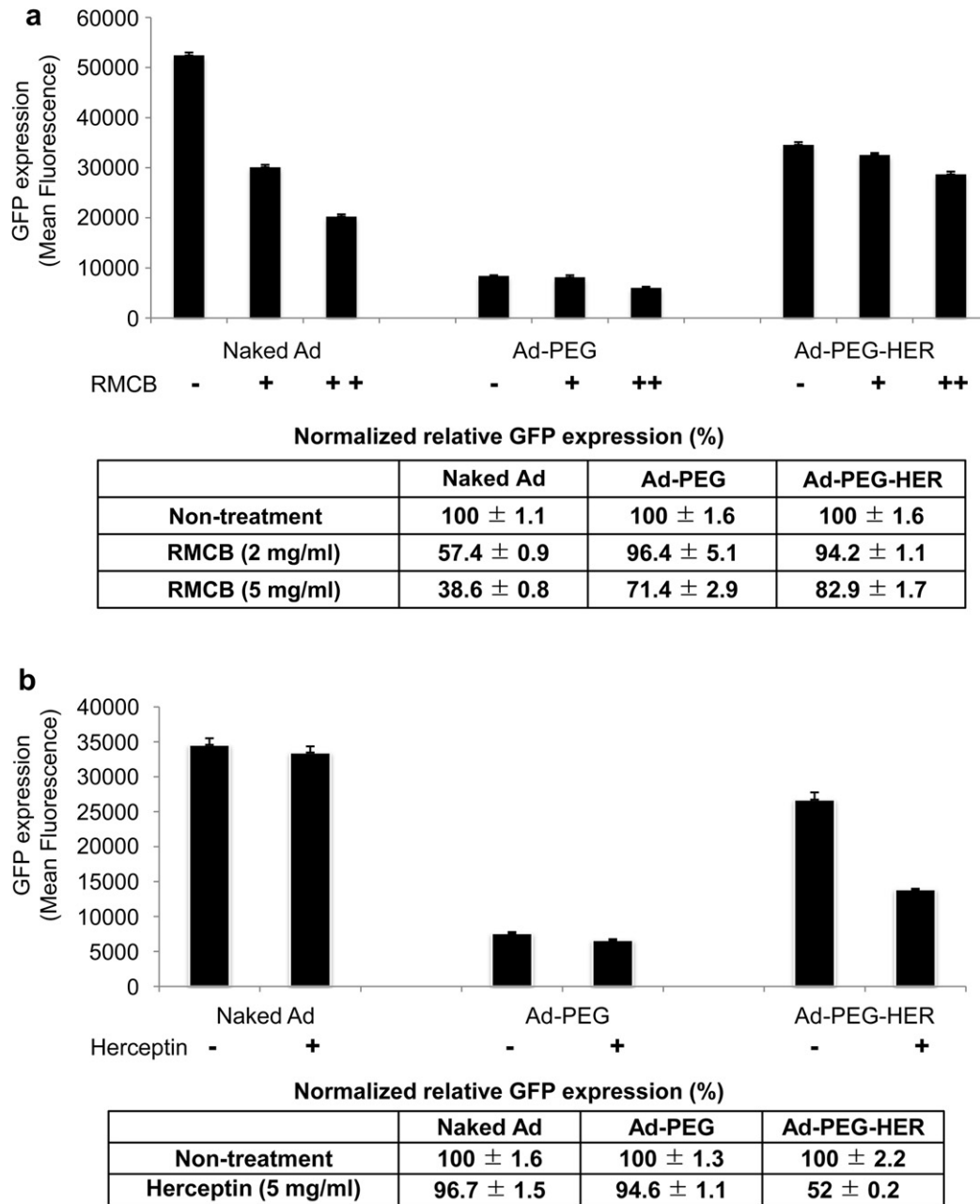


Fig. 2. Transduction of SK-OV3 cells with naked Ad, Ad-PEG, or Ad-PEG-HER in the presence and absence of Ab specific to CAR (A) or Her2/neu (B). SK-OV3 cells were pre-incubated for 1 h at 4 °C with CAR-specific Ab (RMCB) (b) or Herceptin(c). Naked Ad, Ad-PEG, or Ad-PEG-HER was then added at an MOI of 200. At 48 h post transduction, cells were analyzed for GFP expression by flow cytometry analysis. The data are representatives of three independent experiments performed in triplicate. Bars represent mean ± SE. Competition assay with Ad fiber protein or Herceptin Ab shows Her2/neu-dependent/CAR-independent uptake of Ad-PEG-HER.

a common feature of cancer cells. Additionally, expression of the relaxin gene increases virus spread throughout a tumor by reducing the extracellular matrix. Both of these properties make DWP418 a potent oncolytic Ad [24,26]. To demonstrate Her2/neu cancer cell-specific killing by PEG-modified DWP418 conjugated to Herceptin (DWP418-PEG-HER), an MTT assay was performed using Her2/neu-positive (SK-OV3 & MDA-MB231) and -negative (SK-Hep1 & IMR90) cell lines treated with naked DWP418, DWP418-PEG, or DWP418-PEG-HER. Naked DWP418 induced potent cell killing in all three cancer cell lines (MDA-MB231, SK-OV3, and SK-Hep1), but not in the IMR90 normal fibroblast cell line, demonstrating that DWP418 is a cancer cell-selective

oncolytic Ad (Fig. 5). DWP418-PEG-HER also had potent oncolytic activity, comparable with naked DWP418, but it was restricted to Her2/neu-positive cancer cell lines. Due to PEGylation and reduced entry, DWP418-PEG achieved only low levels of cytotoxicity in all cell lines tested. Of interest, DWP418-PEG-HER treatment was much less cytotoxic than DWP418-PEG treatment for Her2/neu-negative SK-Hep1 cells, suggesting that conjugation with Herceptin may have provided additional protection against non-target cells oncolytic activity. Together, these data demonstrate that PEG-modified oncolytic Ad conjugated with Herceptin specifically killed Her2/neu-expressing cancer cells, mediated by the interaction between Her2/neu and Herceptin.

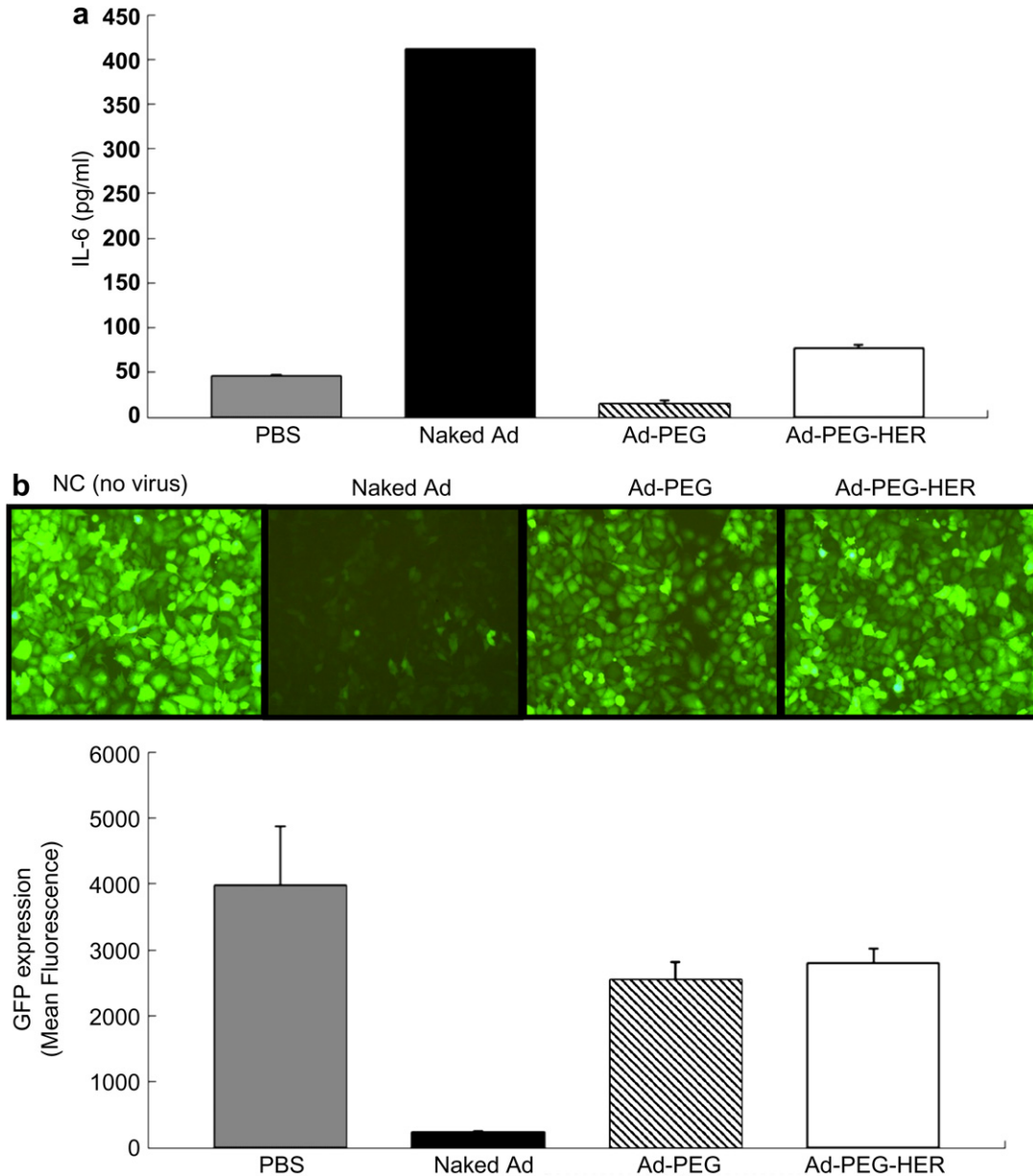


Fig. 3. Assessment of innate and humoral immune response against PEGylated Ads. (a) Induction of IL-6 inflammatory cytokine. At 6 h after intravenous injection of 1×10^{10} VP naked Ad, Ad-PEG, or Ad-PEG-HER into mice, serum was collected and IL-6 levels were measured by ELISA. (b) Influence of neutralizing antiserum on transduction efficiency of GFP-expressing Ad. At 14 days post 2nd systemic injection of 1×10^{10} VP naked Ad, Ad-PEG, or Ad-PEG-HER into mice, serum diluted 1:50 was pre-incubated for 20 min at 37 °C with dE1/GFP, and then applied to U343 cells. Then, the cells were incubated for 48 h followed by observation of GFP fluorescence by microscopy. The data presented are means and SE of the means ($n = 3$) of three representative experiments.

3.5. DWP418-PEG-HER has greater antitumor activity than non-targeted oncolytic Ad in a murine xenograft model

To evaluate the therapeutic efficacy of the Her2/neu-targeted DWP418-PEG-HER, the growth of Her2/neu-positive xenograft tumors was determined following treatment with each Ad preparation. Her2/neu-positive xenograft tumors were established and then the mice were treated by intravenous injection with PBS, naked DWP418, DWP-PEG, or DWP418-PEG-HER. Growth of the tumors was then compared (Fig. 6 a). Treatment with DWP418-PEG-HER resulted in significantly greater antitumor activity than treatment with naked DWP418 or DWP418-PEG in both Her2/neu-positive SK-OV3 and MDA-MB435 xenografts. For SK-OV3 tumors at 30 post treatment, tumors were 285 ± 64 , 267 ± 87 , and

$66 \pm 27 \text{ mm}^3$ for naked DWP418, DWP418-PEG, and DWP418-PEG-HER, respectively and represented a statistically significant inhibition of tumor growth compared to the PBS-treated control group ($816 \pm 248 \text{ mm}^3$) ($P < 0.05$). Similar antitumor activity was observed 60 days after treatment for the MDA-MB435 xenografts, tumors were 2421 ± 455 , 1774 ± 793 , and $1186 \pm 355 \text{ mm}^3$ for naked DWP418, DWP418-PEG, or DWP418-PEG-HER, respectively, and were in all cases lower than in the PBS-treated control group ($2715 \pm 686 \text{ mm}^3$). Further, in the SK-OV3 model, DWP418-PEG-HER treatment increased the survival time of approximately 67% ($P < 0.01$) compared with the other groups, and a similar trend was observed in the MDA-MB435 model.

Of interest, the antitumor activity of DWP418-PEG was equivalent to and better than naked DWP418 in the SK-OV3 and

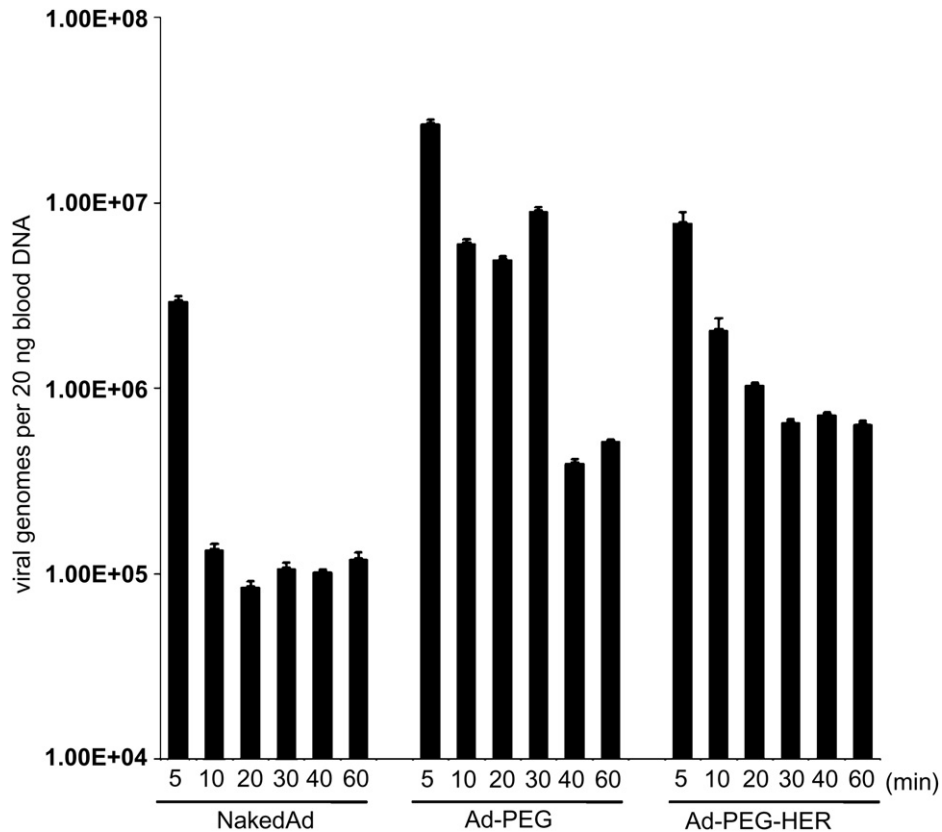


Fig. 4. Pharmacokinetics of Her2/neu-targeted and PEG-modified Ad. Naked Ad, Ad-PEG, or Ad-PEG-HER (1×10^{10} VP) was injected intravenously into mice and blood samples were taken at several time points and Ad genome copy number was determined by real-time quantitative PCR. Blood circulation time for Ad-PEG and Ad-PEG-HER was significantly increased compared with naked Ad.

MDA-MB435 models, respectively, though DWP418-PEG showed very minimal cytotoxicity *in vitro*. It is possible that DWP418-PEG preferentially accumulated in tumors by enhanced permeability and retention (EPR) effect-mediated passive targeting. DWP418-PEG-HER showed greater antitumor activity than DWP418-PEG in Her2/neu-positive cells, indicating Her2/neu-targeting led to active targeting tumor killing, but could also have some degree of passive-targeting tumor killing activity. To assess this, the antitumor activity of each preparation against Her2/neu-negative MCF7-mot breast xenograft tumors was assessed. Both DWP418-PEG and DWP418-PEG-HER elicited equivalent antitumor efficacy (Fig. 6 b), demonstrating that only passive-targeting tumor killing occurred due to the lack of the Her2/neu tumor antigen in this model.

3.6. Biodistribution of Her2/neu-targeted and PEG-modified oncolytic Ad in tumor-bearing mice

To evaluate the benefits of oncolytic Ad-PEGylation for efficient *in vivo* tumor delivery, biodistribution studies were carried out. Mice bearing MDA-MB435 subcutaneous tumors were treated intravenously three times every other day with each oncolytic Ad preparation (1×10^{10} VP), and 24 h after injection the heart, stomach, liver, kidney, muscle, lung, and tumor tissues were harvested and the level of Ad DNA in each tissue determined by real-time quantitative PCR (Fig. 7 a). The uptake of PEGylated Ads group (DWP418-PEG and DWP418-PEG-HER) in liver was significantly lower than naked Ad, showing 2.0×10^4 - and 3.7×10^5 -fold less accumulation in liver, respectively. The PEGylated Ad level was also lower than naked Ad in most of the other tissues examined. In

contrast, DWP418-PEG and DWP418-PEG-HER accumulated in the tumor tissue at 7.7×10^2 - and 5.8×10^4 -fold higher levels than naked Ad, respectively. Consequently, the liver to tumor ratio increased from $1:1 \times 10^{-6}$ for naked DWP418 to 1:15 and 1:21,560 for DWP418-PEG and DWP418-PEG-HER, respectively. This represents a 10^7 -fold (DWP418-PEG) and 10^{10} -fold (DWP418-PEG-HER) increase in the liver to tumor bioaccumulation ratio for the PEGylated Ad compared to naked Ad.

We confirmed the real-time PCR results by detecting the Ad E1A antigen by immunohistochemistry. Viral particles were more abundant in tumor tissues from mice treated with DWP418-PEG or DWP418-PEG-HER than those treated with naked DWP418 (Fig. 7 a), with DWP418-PEG-HER being distributed widely throughout the tumor tissue, indicating a broader tumor-targeting capacity. In contrast, detection of E1A and relaxin gene expression in the liver of mice treated with naked Ad was substantially higher than mice treated with DWP418-PEG or DWP418-PEG-HER (Fig. 7 b).

3.7. *In vivo* hepatotoxicity of intravenously injected Ad-PEG-HER

The lack of liver accumulation of Ad-PEG-HER indicated this vector may show reduced liver toxicity compared to naked Ad. To assess hepatotoxicity associated with Ad injection, serum alanine aminotransferase (ALT) and aspartate aminotransferase (AST) levels were determined after intravenous administration of naked DWP418, DWP418-PEG, or DWP418-PEG-HER (Fig. 8 a). Mice treated with naked DWP418 had significantly higher serum transaminase levels 3 days after injection than PBS controls ($P < 0.05$). In contrast, no significant increase in ALT and AST levels were

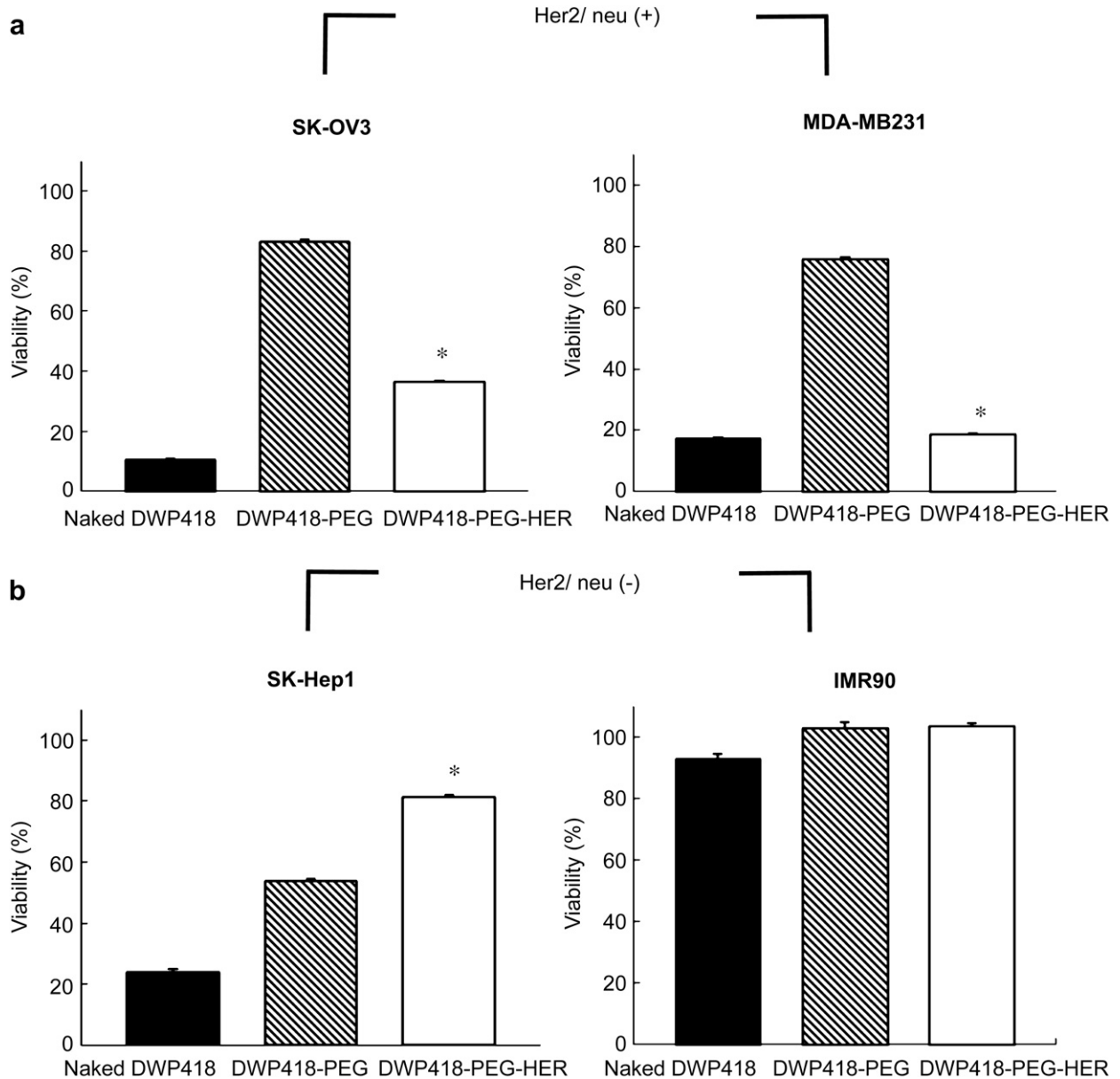


Fig. 5. Her2/neu-specific cell killing efficacy of DWP418-PEG-HER. Her2/neu-positive (a) and -negative (b) cells were infected with naked DWP418, DWP418-PEG, or DWP418-PEG-HER. At 4 days post infection, cell viability was determined by an MTT assay. PEG-modified oncolytic Ad conjugated with Herceptin induced specific killing in a Her2/neu-dependent manner. Each data point represents the mean of triplicate infected cultures. * $P < 0.01$ versus cells infected with DWP418-PEG.

observed in mice treated with either DWP418-PEG or DWP418-PEG-HER. Further, histopathology analysis of hematoxylin-eosin stained liver sections demonstrated that PEGylated Ad-treated mice did not display typical Ad-associated hepatic injury (Fig. 8 b). In the livers of naked Ad-treated mice, acidophilic cytoplasm (upper) and nuclei degeneration (mitosis, no nuclei and dinuclei) was observed. No hepatic injury-related morphological abnormalities were detected in DWP418-PEG- or DWP418-PEG-HER-treated animals. These data indicate that PEGylation of Ad reduced Ad-associated liver toxicity.

4. Discussion

Use of gene therapy viral vectors to treat metastatic cancer requires the virus to target tumor cells that have disseminated

throughout the patient. This requires an extended circulation time in the plasma without vector depletion through infection of normal non-target cells [27]. Approaches to increase plasma retention time have involved genetic modification to eliminate Ad tropism for its normal cellular receptors, (CAR) or integrins $\alpha v \beta 3$ and $\alpha v \beta 5$ [28–31], and nonspecific surface masking of Ad with PEG. PEGylation of Ad increases plasma retention time and reduces Ad immunogenicity, but results in a loss of transduction efficiency caused by PEG blocking specific Ad fiber-cellular receptor interactions [32,33]. Our data demonstrate the specific retargeting of a PEGylated oncolytic Ad through conjugation with Herceptin, a Her2/neu-specific monoclonal antibody, which has already been approved for treatment of Her2/neu-positive breast cancer.

Systemic delivery of Ad induces a strong innate immune response and is a major disadvantage for the use of Ad vectors in

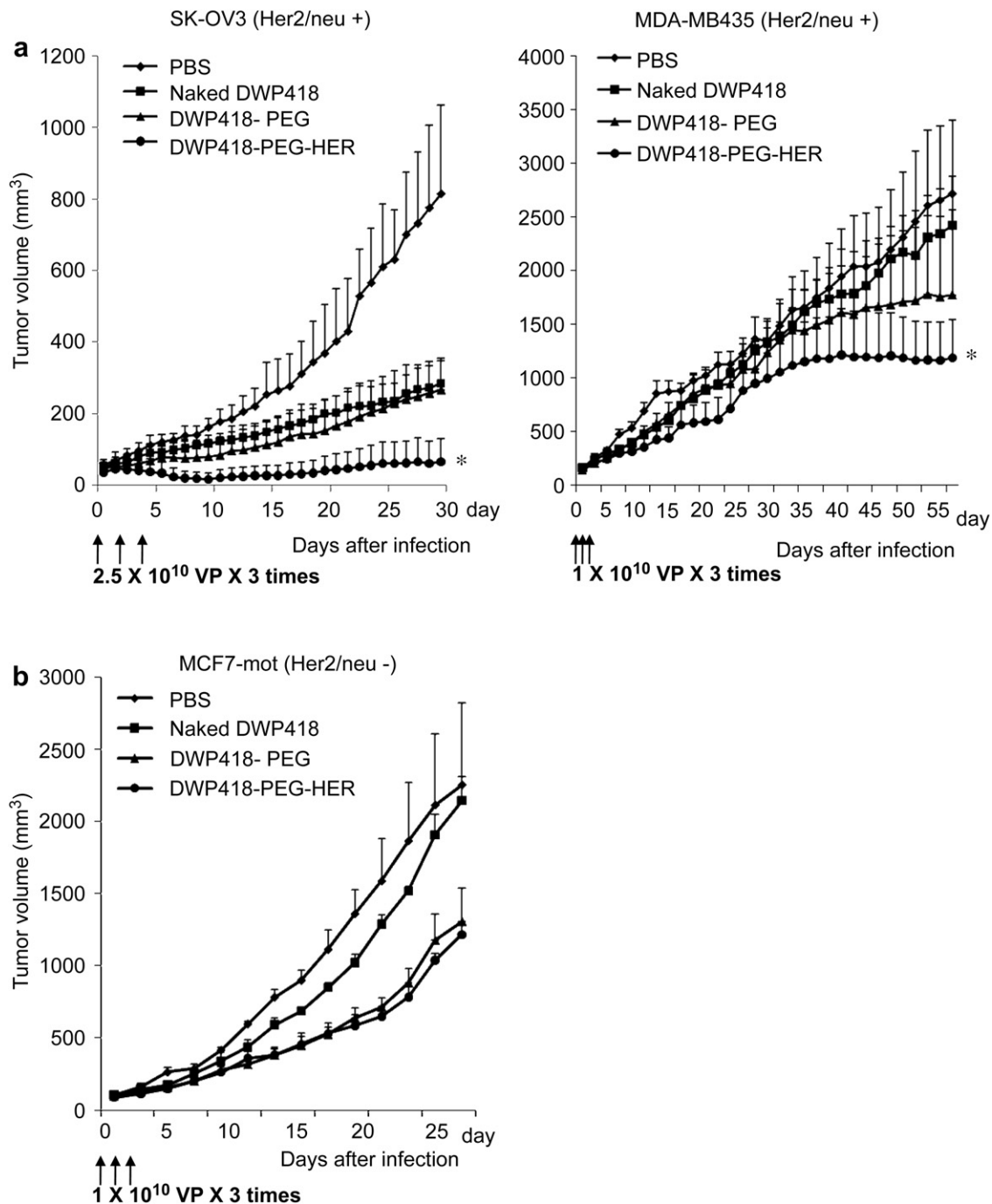


Fig. 6. Antitumor efficacy of naked DWP418, DWP418-PEG, and DWP418-PEG-HER. Her2/neu-positive (SK-OV3 ($n = 5$) and MDA-MB435 ($n = 6$)) and -negative (MCF7-mot ($n = 3$)) xenografts were established in nude mice. Once the tumor size was 100–120 mm³, each Ad formulation was intravenously administered three times every other day. Data represent means \pm SE. * $P < 0.05$ versus DWP418-PEG-treated tumors.

gene therapy [34]. Ad capsid proteins activate several kinase pathways within minutes of intravenous injection and induce the production of proinflammatory chemokines and cytokines [35,36]. Since IL-6 is well established as a major inflammatory cytokines induced by systemic delivery of Ad, we assessed plasma levels of IL-6 at 6 h post Ad injection. We selected a single 6-h time point because in the mouse model, inflammatory cytokines peak at approximately 6 h after virus injection and rapidly decline to baseline values by 24 h [7]. PEGylation of Ad significantly reduced the plasma level of IL-6 elicited by the Ad, implying that PEGylation

may attenuate the trigger for the proinflammatory signalling cascades by masking molecular immunogenic epitopes or patterns on the Ad capsid (Fig. 3 a). Further, PEGylation also decreased the induction of Ad-specific neutralizing antibodies by 70–74% (Fig. 3 b). The presence of Ad-neutralizing antibodies inactivates the vector, reduces gene transfer, and prevents the same vector from being used for multiple doses. PEGylation, even in the context of the Herceptin-conjugated Ad, substantially reduced immunogenicity. Thus, this method is a feasible platform for the development of a systemic multi-dose, targeted gene therapy/oncolytic vectors.

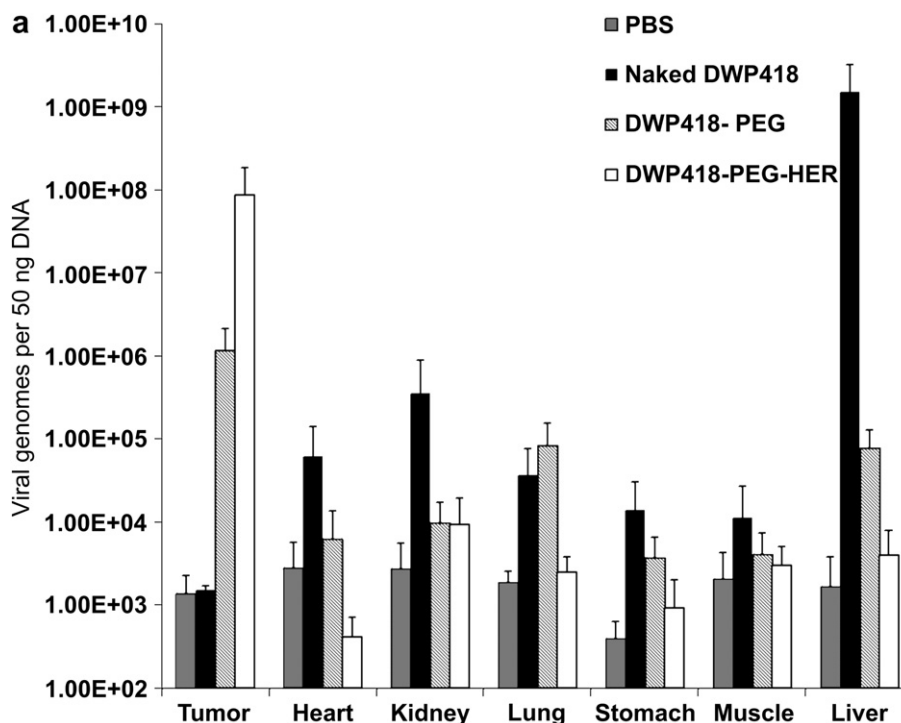


Fig. 7. Biodistribution of Her2/neu-targeted and PEG-modified oncolytic Ad in tumor-bearing mice. 1×10^{10} VP of naked DWP418, DWP418-PEG, or DWP418-PEG-HER was systemically injected three times every other day into the tail vein of the mice. (a) The heart, kidney, lung, stomach, muscle, liver, and tumor tissues were harvested 24 h post-injection and real-time quantitative PCR was performed to detect Ad genomes. Data are expressed as copy number of Ad E1A gene. Data represent means \pm SE and $n = 3$ for each experimental condition. (b) Representative photographs of Ad E1A immunohistochemistry in the tumor tissues. More abundant Ad particles were detected in the tumor tissue of mice injected with DWP418-PEG-HER compared with those treated with either naked DWP418 or DWP418-PEG. (c) Representative photographs of Ad E1A and relaxin immunohistochemistry in the liver tissue.

The mechanism of the PEG-mediated reduction in immunogenicity remains to be fully determined. Ad capsid proteins (hexon, fiber, and penton) are potent immune system inducers and the primary targets of reactive PEGs [10]. Thus, masking the viral capsid proteins with PEG may blunt the immune response, and PEGylation reduces the phagocytosis of Ad by macrophages and Kupffer cells, which are involved in the initial activation of both innate and adaptive immune responses [7,8].

Treatment of disseminated metastases by Ad vectors requires the retention time of Ad in the blood to be prolonged. Our results show that PEGylated Ads (Ad-PEG & Ad-PEG-HER) injected intravenously into mice had an increased blood circulation time that was 45-fold and 16-fold greater than naked Ad, at 1 h after injection. Similarly, Gao et al. previously reported that the plasma half-life of PEGylated Ads, with 90% and 100% modification, was increased from 1.9 min (unmodified Ad) to 6.4 and 22 min, respectively [32]. These data are consistent with other studies using a variety of PEGylated drug delivery systems. It is thought that PEG conjugation forms a steric barrier that dramatically reduces serum protein adsorption, prevents the attraction of opsonins, and prevents uptake by reticuloendothelial system (RES) [37–39]. Further, naked Ad is rapidly accumulated in the liver after intravenous injection due to capture by Kupffer cells and hepatocytes, which express high levels of Ad receptors. Therefore, reduced Kupffer cell uptake by physical masking of Ad results in a longer blood circulation time and therefore improved chance for interaction with target cancer cells.

Using the PEGylated/Herceptin-conjugated Ad system, we sought to develop a targeted antitumor vector based on the relaxin-expressing oncolytic Ad DWP418. *In vitro*, DWP418-PEG-HER showed Her2/neu-dependent oncolytic activity, indicating

that the Herceptin targeting moiety directed selective entry of this vector into Her2/neu-positive cells (Fig. 5). *In vivo*, DWP418-PEG-HER had greater antitumor activity against Her2/neu-positive SK-OV3 and MDA-MB435 xenograft tumors than naked DWP418 and DWP418-PEG, but equivalent antitumor activity as DWP418-PEG against Her2/neu-negative MCF7-mot tumors. Thus the enhanced antitumor activity of DWP418-PEG-HER in Her2/neu-positive is based upon active targeting of the vector to the tumor through the specific interaction between Herceptin and cell surface Her2/neu (Fig. 6).

DWP418-PEG induced equivalent or better antitumor efficacy than naked Ad in both Her2/neu-positive and -negative tumors, even though DWP418-PEG showed negligible killing efficacy *in vitro*. The antitumor effect of DWP418-PEG is likely due to the increased circulation time of PEGylated Ad compared with naked Ad. Hypervascular permeability and impaired lymphatic drainage of tumor tissue facilitate extravasation of macromolecules, like DWP418-PEG, resulting in preferential accumulation in solid tumor tissues [9]. Accumulated DWP418-PEG in tumor tissues would be efficiently, but non-specifically, internalized into cells due to the elevated rate of endocytosis of tumor cells. This model is supported by the observed 770-fold increase in Ad-PEG detected in the tumor tissues compared to naked Ad (Fig. 7).

Specific targeting of DWP418-PEG-HER to tumor cells with Herceptin led to a 58,000-fold higher accumulation of virus than in tumors of mice treated with naked Ad. This increase in virus accumulation in tumors is much greater than the previous report by Gao et al [9,32]. The enhanced accumulation after treatment with DWP418-PEG-HER is likely due to efficient secondary infection of tumor cells by progeny DWP418, since previous studies used replication-deficient vectors. Further, no apparent toxicity was

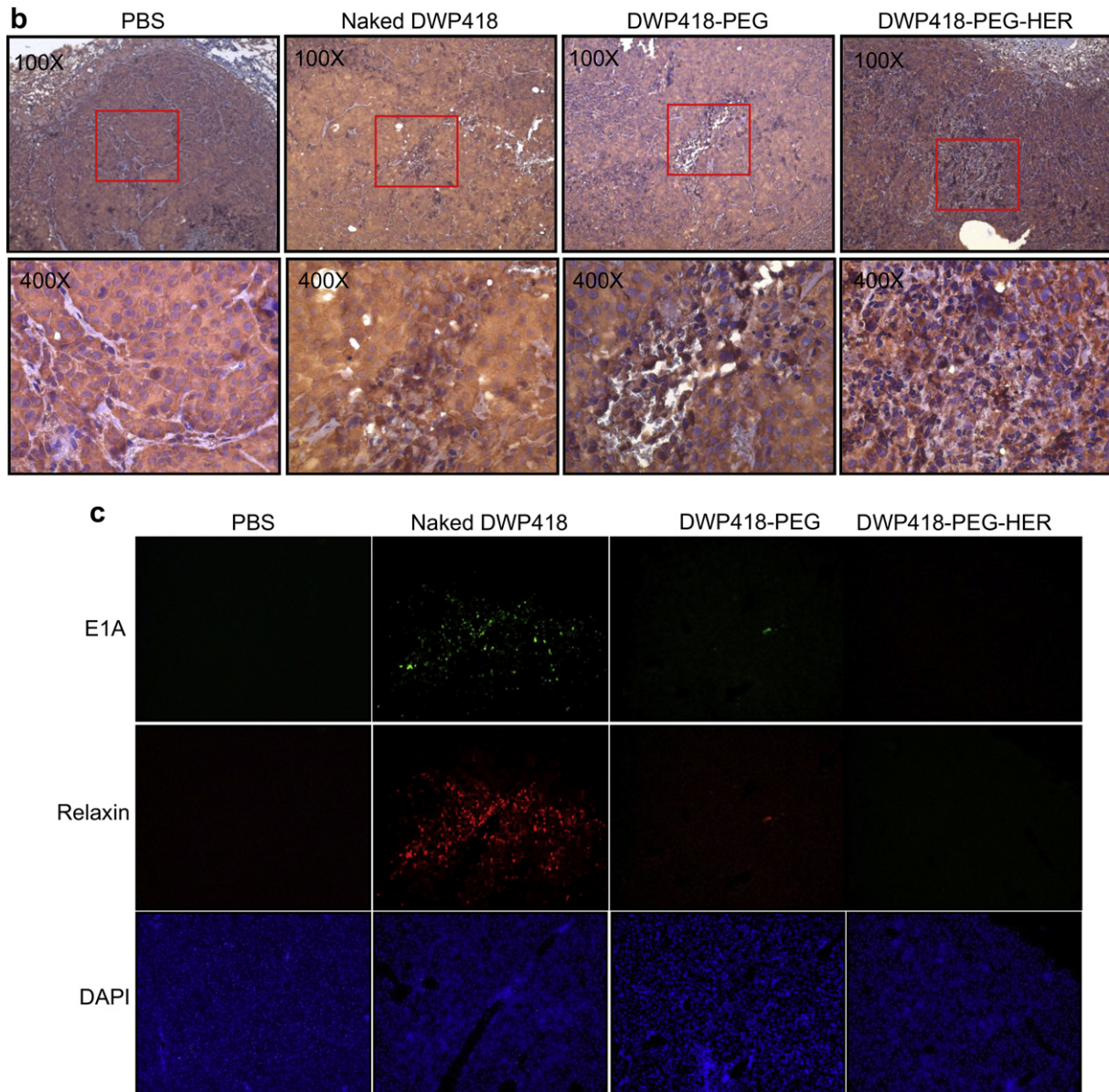


Fig. 7. (continued).

noted in animals that received DWP418-PEG or DWP418-PEG-HER during the course of this study. Ad-related liver toxicity, as measured by serum ALT and AST levels, was absent in PEGylated Ad-treated animals. Further, no histological abnormalities were observed in these livers, which correlates with the 2.0×10^4 - and 3.7×10^5 -fold less DWP418-PEG and DWP418-PEG-HER detected, respectively.

Overall, the liver to tumor biodistribution ratio for DWP418-PEG and DWP418-PEG-HER were 10^7 - and 10^{10} -fold greater than naked DWP418. Thus, the increased distribution of E1A staining in the DWP418-PEG-HER-treated tumors and lower liver accumulation demonstrated that PEGylation and Herceptin directed accumulation in the tumor beds, tumor-specific replication through the TERT promoter limited lytic replication to cancer cells, and expression of relaxin promoted secondary spread of the virus. These biodistribution data underline several important characteristics of this vector system. First, oncolytic Ad can be successfully encapsulated by biocompatible polymers like PEG that allow

systemic delivery through intravenous administration. Second, significant secondary amplification of oncolytic Ad is induced after tumor-selective accumulation in the tumor tissue, potentiating of the therapeutic efficacy. Third, selective restriction of Ad replication to cancer cells limits the potential toxicity to normal tissues. Fourth, the significantly lower liver accumulation reduced Ad-associated liver toxicity, which is the major side effect of Ad vectors used clinically.

A tumor-targeting vector system that can be delivered intravenously and can effectively treat both primary and metastatic lesions is needed. We believe that biocompatible polymer molecules, like PEG, could negate the limitations of conventional Ad vectors, such as hepatotoxicity, immunogenicity, and short blood circulation time, and allow the development of specific targeting platforms for tumor-selective oncolytic therapies. The data presented here demonstrate that tumor-targeting PEGylated oncolytic Ads have potential for effective and safe systemic therapies to treat both primary and metastatic tumors.

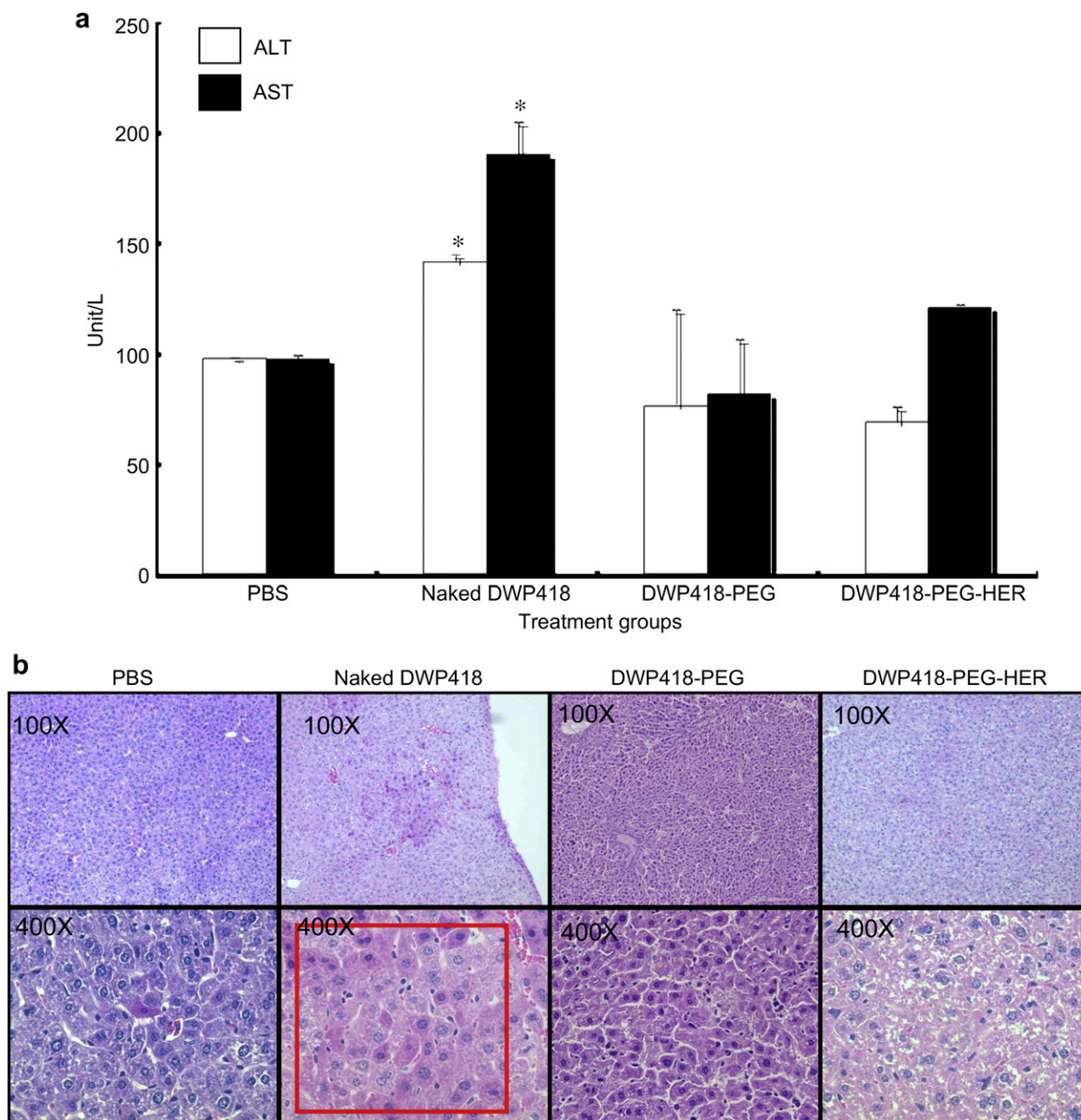


Fig. 8. Assessment of hepatotoxicity of PEG-conjugated Ads. (a) Measurement of serum ALT and AST 72 h following intravenous administration of 1×10^{10} VP of DWP418, DWP418-PEG, or DWP418-PEG-HER. Data represent means \pm SE and $n = 3$ for each experimental condition. (b) Assessment of liver histopathology. Photomicrographs of representative H&E-stained mouse livers 24 h after intravenous injection of each Ad preparation.

5. Conclusion

Ad targeting platform based on the conjugation of a polymer and targeting moiety onto Ad was developed to overcome typical restrictions in virus vector targeting for systemic administration. Herceptin-conjugated and PEGylated Ad showed longer circulation times and decreased neutralizing antibody and IL-6 induction than naked Ad, demonstrating that PEG conjugation can reduce the immune response against Ad and enhance the vector's blood circulation profile. Moreover, Her2/neu-targeted and PEGylated oncolytic Ad (DWP418-PEG-HER) had greater antitumor activity against Her2/neu-positive tumors than naked DWP418 or PEGylated DWP418 (DWP418-PEG). Further, the antitumor activity of DWP418-PEG-HER was equivalent to the non-targeted DWP418-

PEG against Her2/neu-negative tumors, demonstrating that the enhanced antitumor efficacy elicited by DWP418-PEG-HER in Her2/neu-positive tumors resulted from active targeting-mediated antitumor killing, mediated by the specific interaction between Herceptin on the surface of the PEGylated Ad and Her2/neu expressed on the tumor cells. In sum, this study demonstrates Ad-mediated active tumor-specific killing efficacy after intravenous injection.

Acknowledgments

This work was supported by grants from the Ministry of Knowledge Economy (10030051, Dr. C-O Yun), the National Research Foundation of Korea (R15-2004-024-02001-0, 2010-0029220,

2009K001644, Dr. C-O Yun), and a faculty research grant (6-2007-0114, Dr. J-H Sohn) from Yonsei University College of Medicine. Pyung-Hwan Kim, Yukyung Jung, and Joung-Woo Choi are graduate students sponsored by NRF through National Core Research Center for Nanomedical Technology, Yonsei University, Seoul, South Korea.

The authors Pyung-Hwan Kim and Joo-Hyuk Sohn contributed equally to this work.

Appendix

Figure with essential color discrimination. Fig. 3 in this article is difficult to interpret in black and white. The full color images can be found in the on-line version, at doi:10.1016/j.biomaterials.2010.10.031.

References

- [1] Kreppel F, Kochanek S. Modification of adenovirus gene transfer vectors with synthetic polymers: a scientific review and technical guide. *Mol Ther* 2008;16:16–29.
- [2] Parato KA, Senger D, Forsyth PA, Bell JC. Recent progress in the battle between oncolytic viruses and tumours. *Nat Rev Cancer* 2005;5:965–76.
- [3] Yun CO. Overcoming the extracellular matrix barrier to improve intratumoral spread and therapeutic potential of oncolytic virotherapy. *Curr Opin Mol Ther* 2008;10:356–61.
- [4] Peng Z. Current status of gene therapy in China: recombinant human Ad-p53 agent for treatment of cancers. *Hum Gene Ther* 2005;16:1016–27.
- [5] Peng Z, Yu Q, Bao L. The application of gene therapy in China. *IDrugs* 2008;11:346–50.
- [6] Raty JK, Pikkarainen JT, Wirth T, Yla-Herttuala S. Gene therapy: the first approved gene-based medicines, molecular mechanisms and clinical indications. *Curr Mol Pharmacol* 2008;1:13–23.
- [7] Mok H, Palmer DJ, Ng P, Barry MA. Evaluation of polyethylene glycol modification of first-generation and helper-dependent adenoviral vectors to reduce innate immune responses. *Mol Ther* 2005;11:66–79.
- [8] Alemany R, Suzuki K, Curiel DT. Blood clearance rates of adenovirus type 5 in mice. *J Gen Virol* 2000;81:2605–9.
- [9] Doronin K, Shashkova EV, May SM, Hofherr SE, Barry MA. Chemical modification with high molecular weight polyethylene glycol reduces transduction of hepatocytes and increases efficacy of intravenously delivered oncolytic adenovirus. *Hum Gene Ther* 2009;20:975–88.
- [10] O'Riordan CR, Lachapelle A, Delgado C, Parkes V, Wadsworth SC, Smith AE, et al. PEGylation of adenovirus with retention of infectivity and protection from neutralizing antibody in vitro and in vivo. *Hum Gene Ther* 1999;10:1349–58.
- [11] Maeda M, Kida S, Hojo K, Eto Y, Gaob JQ, Kurachi S, et al. Design and synthesis of a peptide-PEG transporter tool for carrying adenovirus vector into cells. *Bioorg Med Chem Lett* 2005;15:621–4.
- [12] Eto Y, Gao JQ, Sekiguchi F, Kurachi S, Katayama K, Maeda M, et al. PEGylated adenovirus vectors containing RGD peptides on the tip of PEG show high transduction efficiency and antibody evasion ability. *J Gene Med* 2005;7:604–12.
- [13] Kreppel F, Gackowski J, Schmidt E, Kochanek S. Combined genetic and chemical capsid modifications enable flexible and efficient de- and retargeting of adenovirus vectors. *Mol Ther* 2005;12:107–17.
- [14] Oh IK, Mok H, Park TG. Folate immobilized and PEGylated adenovirus for retargeting to tumor cells. *Bioconjug Chem* 2006;17:721–7.
- [15] Ogawara K, Kuldo JM, Oosterhuis K, Kroesen BJ, Rots MG, Trautwein C, et al. Functional inhibition of NF-kappaB signal transduction in alphavbeta3 integrin expressing endothelial cells by using RGD-PEG-modified adenovirus with a mutant IkappaB gene. *Arthritis Res Ther* 2006;8:R32.
- [16] Eto Y, Yoshioka Y, Asavatanabodee R, Mizuguchi H, Mukai Y, Okada N, et al. Development of pegylated adenovirus vector for cancer gene therapy. *Yakugaku Zasshi* 2008;128:1733–42.
- [17] Lanciotti J, Song A, Doukas J, Sosnowski B, Pierce G, Gregory R, et al. Targeting adenoviral vectors using heterofunctional polyethylene glycol FGF2 conjugates. *Mol Ther* 2003;8:99–107.
- [18] Ogawara K, Rots MG, Kok RJ, Moorlag HE, Van Loenen AM, Meijer DK, et al. A novel strategy to modify adenovirus tropism and enhance transgene delivery to activated vascular endothelial cells in vitro and in vivo. *Hum Gene Ther* 2004;15:433–43.
- [19] Slamon DJ, Clark GM, Wong SG, Levin WJ, Ullrich A, McGuire WL. Human breast cancer: correlation of relapse and survival with amplification of the HER-2/neu oncogene. *Science* 1987;235:177–82.
- [20] Slamon DJ, Leyland-Jones B, Shak S, Fuchs H, Paton V, Bajamonde A, et al. Use of chemotherapy plus a monoclonal antibody against HER2 for metastatic breast cancer that overexpresses HER2. *N Engl J Med* 2001;344:783–92.
- [21] Smith I, Procter M, Gelber RD, Guillaume S, Feyereislova A, Dowsett M, et al. 2-year follow-up of trastuzumab after adjuvant chemotherapy in HER2-positive breast cancer: a randomised controlled trial. *Lancet* 2007;369:29–36.
- [22] Piccart-Gebhart MJ, Procter M, Leyland-Jones B, Goldhirsch A, Untch M, Smith I, et al. Trastuzumab after adjuvant chemotherapy in HER2-positive breast cancer. *N Engl J Med* 2005;353:1659–72.
- [23] Jung Y, Park HJ, Kim PH, Lee J, Hyung W, Yang J, et al. Retargeting of adenoviral gene delivery via herceptin-PEG-adenovirus conjugates to breast cancer cells. *J Control Release* 2007;123:164–71.
- [24] Kim E, Kim JH, Shin HY, Lee H, Yang JM, Kim J, et al. Ad-mTERT-delta19, a conditional replication-competent adenovirus driven by the human telomerase promoter, selectively replicates in and elicits cytopathic effect in a cancer cell-specific manner. *Hum Gene Ther* 2003;14:1415–28.
- [25] Kim J, Cho JY, Kim JH, Jung KC, Yun CO. Evaluation of E1B gene-attenuated replicating adenoviruses for cancer gene therapy. *Cancer Gene Ther* 2002;9:725–36.
- [26] Kim JH, Lee YS, Kim H, Huang JH, Yoon AR, Yun CO. Relaxin expression from tumor-targeting adenoviruses and its intratumoral spread, apoptosis induction, and efficacy. *J Natl Cancer Inst* 2006;98:1482–93.
- [27] Green NK, Herbert CW, Hale SJ, Hale AB, Mautner V, Harkins R, et al. Extended plasma circulation time and decreased toxicity of polymer-coated adenovirus. *Gene Ther* 2004;11:1256–63.
- [28] Alemany R, Curiel DT. CAR-binding ablation does not change biodistribution and toxicity of adenoviral vectors. *Gene Ther* 2001;8:1347–53.
- [29] Leissner P, Legrand V, Schlesinger Y, Hadji DA, van Raaij M, Cusack S, et al. Influence of adenoviral fiber mutations on viral encapsidation, infectivity and in vivo tropism. *Gene Ther* 2001;8:49–57.
- [30] Einfeld DA, Schroeder R, Roelvink PW, Lizonova A, King CR, Kovsed I, et al. Reducing the native tropism of adenovirus vectors requires removal of both CAR and integrin interactions. *J Virol* 2001;75:11284–91.
- [31] Yun CO, Yoon AR, Yoo JY, Kim H, Kim M, Ha T, et al. Coxsackie and adenovirus receptor binding ablation reduces adenovirus liver tropism and toxicity. *Hum Gene Ther* 2005;16:248–61.
- [32] Gao JQ, Eto Y, Yoshioka Y, Sekiguchi F, Kurachi S, Morishige T, et al. Effective tumor targeted gene transfer using PEGylated adenovirus vector via systemic administration. *J Control Release* 2007;122:102–10.
- [33] Eto Y, Yoshioka Y, Mukai Y, Okada N, Nakagawa S. Development of PEGylated adenovirus vector with targeting ligand. *Int J Pharm* 2008;354:3–8.
- [34] Bangari DS, Mittal SK. Current strategies and future directions for eluding adenoviral vector immunity. *Curr Gene Ther* 2006;6:215–26.
- [35] Elkon KB, Liu CC, Gall JG, Trevejo J, Marino MW, Abrahamson KA, et al. Tumor necrosis factor alpha plays a central role in immune-mediated clearance of adenoviral vectors. *Proc Natl Acad Sci U S A* 1997;94:9814–9.
- [36] Zaiss AK, Liu Q, Bowen GP, Wong NC, Bartlett JS, Muruve DA. Differential activation of innate immune responses by adenovirus and adeno-associated virus vectors. *J Virol* 2002;76:4580–90.
- [37] Inada Y, Furukawa M, Sasaki H, Kodera Y, Hiroto M, Nishimura H, et al. Biomedical and biotechnological applications of PEG- and PM-modified proteins. *Trends Biotechnol* 1995;13:86–91.
- [38] Tsutsumi Y, Tsunoda S, Kaneda Y, Kamada H, Kihira T, Nakagawa S, et al. In vivo anti-tumor efficacy of polyethylene glycol-modified tumor necrosis factor-alpha against tumor necrosis factor-resistant tumors. *Jpn J Cancer Res* 1996;87:1078–85.
- [39] Shibata H, Yoshioka Y, Ikemizu S, Kobayashi K, Yamamoto Y, Mukai Y, et al. Functionalization of tumor necrosis factor-alpha using phage display technique and PEGylation improves its antitumor therapeutic window. *Clin Cancer Res* 2004;10:8293–300.